

Unusual temperature-dependent exchange interaction in $\text{GdFe}_2\text{Al}_{10}$ in comparison with $\text{GdRu}_2\text{Al}_{10}$

M. Sera,¹ H. Nohara,¹ M. Nakamura,¹ H. Tanida,¹ T. Nishioka,² and M. Matsumura²

¹Department of ADSM, Hiroshima University, Higashi-Hiroshima 739-8530, Japan

²Graduate School of Integrated Arts and Science, Kochi University, Kochi 780-8520, Japan

(Received 19 July 2013; published 13 September 2013)

We investigated the magnetic properties of the antiferromagnetic (AFM) compound $\text{GdT}_2\text{Al}_{10}$ ($T = \text{Ru}$ and Fe). Although $\text{GdRu}_2\text{Al}_{10}$ could be understood well as a simple AFM compound, the exchange interaction in $\text{GdFe}_2\text{Al}_{10}$ is found to be greatly varied with temperature. The magnitude of the AFM exchange interaction is reduced with decreasing temperature. We ascribed its origin to the exchange enhancement of the Fe ion with a decrease of temperature as was observed in $\text{YFe}_2\text{Al}_{10}$. The ordered moment is found to be along the $[011]$ direction in the bc plane in both compounds from the anisotropic magnetic susceptibility. The origin of the magnetic anisotropy below T_N could not be understood by the magnetic dipole interaction, which might come from the AFM order on the zigzag chain.

DOI: 10.1103/PhysRevB.88.100404

PACS number(s): 75.30.Et, 75.30.Gw

The Kondo semiconductors $\text{CeT}_2\text{Al}_{10}$ ($T = \text{Ru}, \text{Os}$) with orthorhombic $\text{YbFe}_2\text{Al}_{10}$ -type structure has attracted considerable interest due to their unusual long-range order.¹⁻⁵ These compounds are the first Kondo semiconductors showing AFM order.^{6,7} In the AFM phase, the AFM alignment of the nearest neighbor (NN) Ce moments on the zigzag chain along the c axis is realized.⁶ The AFM order is accompanied by a large spin gap and charge gap.⁸⁻¹⁰ Their origins have not yet been clarified. One of the most unusual properties of these compounds is the magnetization easy axis along the c axis below T_0 . This is not consistent with the magnetic anisotropy of $\chi_a \gg \chi_c \gg \chi_b$ above T_0 . χ_a , χ_b , and χ_c are the magnetic susceptibilities along the three crystal axes. This is in contrast with the normal magnetic anisotropy in $\text{NdT}_2\text{Al}_{10}$. In these compounds, the experimental results strongly suggest $m_{\text{AF}} \parallel a$, consistent with $\chi_a > \chi_c > \chi_b$ in the paramagnetic region.^{11,12} Here, m_{AFM} is the AFM ordered moment. Furthermore, a quite strange spin-flop transition from $m_{\text{AFM}} \parallel c$ to $\parallel b$ for $H \parallel c$ takes place at $4T$.^{13,14} Although the anisotropic c - f hybridization was proposed as the origin of the unusual magnetic anisotropy in the AFM phase, the microscopic mechanism has not been clarified.¹²⁻¹⁶ On the other hand, $\text{CeFe}_2\text{Al}_{10}$ is the intermediate valence compound without showing the magnetic order. The Fe ion contributes to the stronger c - f hybridization than that in $\text{CeT}_2\text{Al}_{10}$ ($T = \text{Ru}$ and Os).¹⁷ Thus, a difference of T ion induces the quite different ground state in $\text{CeT}_2\text{Al}_{10}$.

Although $\text{CeT}_2\text{Al}_{10}$ has been studied extensively, reports on the $\text{LnT}_2\text{Al}_{10}$ ($\text{Ln} = \text{rare-earth atom}$) system are very few. At the early stage, systematic studies using polycrystals were performed by Thiede *et al.*¹ Recently, we reported the detailed study of the structure parameters of $\text{LnT}_2\text{Al}_{10}$ ($T = \text{Ru}$ and Fe).¹⁸ Macroscopic properties of $\text{LnRu}_2\text{Al}_{10}$ ($\text{Ln} = \text{Pr}, \text{Nd}$, and Gd) and $\text{LnOs}_2\text{Al}_{10}$ ($\text{Ln} = \text{Pr}, \text{Nd}, \text{Sm}$, and Gd) have been reported.^{11,12,19-21} Neutron diffraction studies of $\text{LnFe}_2\text{Al}_{10}$ ($\text{Ln} = \text{Tb}, \text{Dy}, \text{Er}$, and Ho) were also reported.²² Although several reports exist, systematic studies of $\text{LnT}_2\text{Al}_{10}$ have not yet been performed. $\text{LnT}_2\text{Al}_{10}$, except for $\text{Ln} = \text{Ce}$ and Yb , is expected to be understood as a normal trivalent rare-earth compound.^{1,18} The crystalline electric field (CEF) splitting is found to be small from the T dependence of χ and the magnetic

ordering temperature is low as expected from the long distance of the nearest neighbor Ln ions (~ 5.2 Å). Here, we note the ferromagnetic instability in close proximity to a quantum critical point of $\text{YFe}_2\text{Al}_{10}$.²³⁻²⁶ It is reported that although $\text{YRu}_2\text{Al}_{10}$, $\text{CeFe}_2\text{Al}_{10}$ and $\text{YbFe}_2\text{Al}_{10}$ exhibit the nonmagnetic ground state, in $\text{YFe}_2\text{Al}_{10}$, exchange enhancement and mass enhancement are observed. This suggests that the Fe ion is located near the boundary between localized and itinerant, and which type of nature appears depends on the Ln ion in $\text{LnFe}_2\text{Al}_{10}$.

In this Rapid Communication, we studied the magnetic properties of $\text{GdT}_2\text{Al}_{10}$ ($T = \text{Ru}$ and Fe) to clarify whether the difference of T ion affects the ground state properties in this system or not as was observed in $\text{YT}_2\text{Al}_{10}$ and also to study the magnetic anisotropy of a Gd ion without an orbital moment.

$\text{GdT}_2\text{Al}_{10}$ ($T = \text{Ru}$ and Fe) single crystals were grown by an Al self-flux method. The magnetic susceptibility was measured by SQUID magnetometry and the low temperature magnetization was measured by a usual extraction method up to 14.5 T.

The temperature (T) dependence of χ and $1/\chi$ of $\text{GdT}_2\text{Al}_{10}$ ($T = \text{Ru}$ and Fe) measured at $H = 0.1$ T are shown in Fig. 1(a). χ_b and χ_c are shown in $\text{GdRu}_2\text{Al}_{10}$ and χ_c in $\text{GdFe}_2\text{Al}_{10}$, respectively. In the paramagnetic region, the T dependence of χ does not depend on the applied field direction in both compounds as expected in Gd compounds. χ_b or χ_c exhibits a sharp peak at 17 K in both compounds, indicating the AFM order below 17 K. We should note that although a difference of χ between $\text{GdRu}_2\text{Al}_{10}$ and $\text{GdFe}_2\text{Al}_{10}$ at high temperatures is small, a large difference appears below 100 K. The increase of χ below 100 K in $\text{GdFe}_2\text{Al}_{10}$ is much larger than that in $\text{GdRu}_2\text{Al}_{10}$. This difference between two compounds is also clearly seen in the temperature dependence of $1/\chi$. In $\text{GdRu}_2\text{Al}_{10}$, $1/\chi_b$ shows a T -linear behavior in the entire temperature region and μ_{eff} is $8.02\mu_B$, close to that expected for a free Gd ion. The paramagnetic Curie temperature θ_p is -16 K whose magnitude is nearly the same as T_N . On the other hand, in $\text{GdFe}_2\text{Al}_{10}$, μ_{eff} is difficult to estimate because a slope of $1/\chi_c$ vs T is varied with temperature, as if the CEF effect exists as is observed in

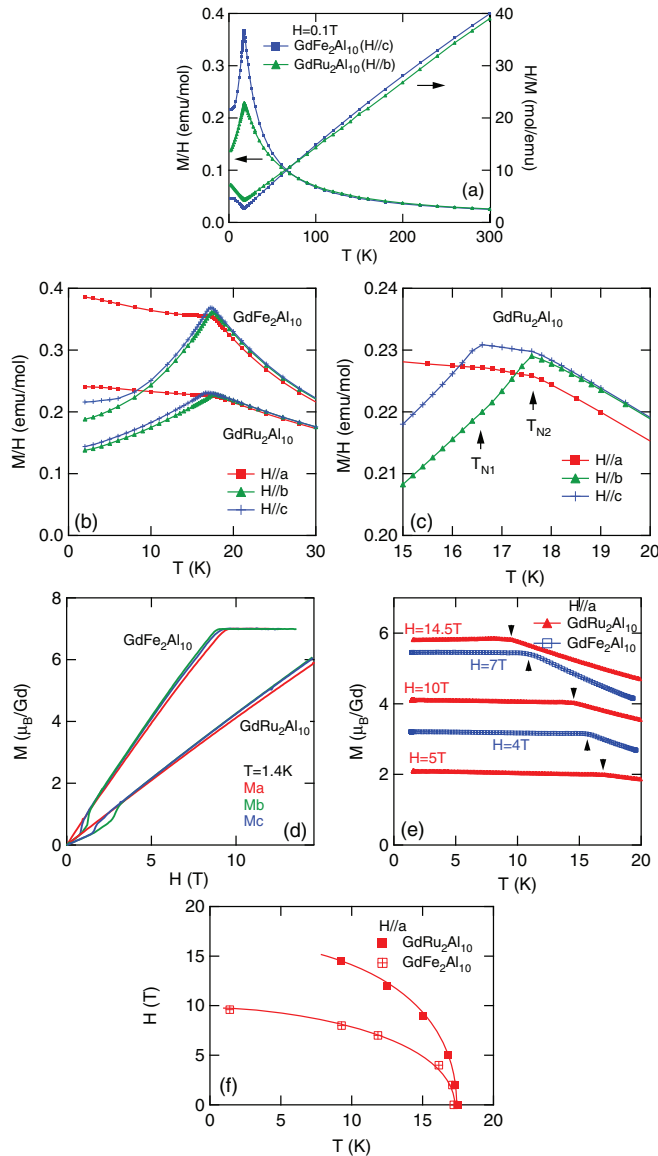


FIG. 1. (Color online) (a) Temperature dependence of χ and $1/\chi$ below 300 K and (b) that of χ along the three crystal axes measured at $H = 0.1$ T, (c) that of χ of $\text{GdRu}_2\text{Al}_{10}$ in an expanded scale around T_N , (d) magnetization curves at $T = 1.4$ K, (e) temperature dependence of M under several magnetic fields, and (f) magnetic phase diagrams of $\text{GdT}_2\text{Al}_{10}$ ($T = \text{Ru}$ and Fe) for $H \parallel a$. The arrows in (e) indicate the transition temperatures. H_{sf} is not drawn and for $T = \text{Ru}$, only higher T_{N2} is shown.

rare-earth compounds with an orbital moment. As a result, θ_p is varied with temperature. θ_p is estimated to be ~ -30 K from a high temperature region but is 0 K below 50 K. As such a T dependent θ_p is not expected in a Gd ion without an orbital moment, the present results indicate the existence of some unknown mechanism in the exchange interaction in $\text{GdFe}_2\text{Al}_{10}$. Its mechanism should be such that the exchange interaction between Gd ions is changed with temperature.

Figures 1(b) and 1(c) show the temperature dependence of χ of $\text{GdT}_2\text{Al}_{10}$ ($T = \text{Ru}$ and Fe) along the three crystal axes at low temperatures and that of $\text{GdRu}_2\text{Al}_{10}$ in an expanded scale around T_N , respectively. Both compounds show similar

magnetic anisotropy. Below T_N , while χ_b and χ_c exhibit a large decrease, χ_a is roughly temperature independent. This means that below T_N , a Gd moment is perpendicular to the a axis and is in the bc plane. The magnitudes of both χ_b and χ_c at $T = 0$ K are roughly half of that at T_N . This suggests that a Gd moment is aligned close to the [011] direction. In $\text{GdFe}_2\text{Al}_{10}$, one transition at $T_N = 17.2$ K is observed and two transition temperatures at $T_{N1} = 16.5$ K and $T_{N2} = 17.6$ K in $\text{GdRu}_2\text{Al}_{10}$ are observed, as shown in Fig. 1(c). From the similar anisotropic T dependence of χ in both compounds, the magnetic structure in the ground state is expected to be the same in these two compounds.

Figures 1(d) and 1(e) show the magnetization curve (M - H) at $T = 1.4$ K and the temperature dependence of M under several magnetic fields of $\text{GdT}_2\text{Al}_{10}$ ($T = \text{Ru}$ and Fe), respectively. The critical field to the paramagnetic region, H_c , is 9 T in $\text{GdFe}_2\text{Al}_{10}$ and is expected to be ~ 17 T in $\text{GdRu}_2\text{Al}_{10}$. In both compounds, a spin-flop transition is seen at $H_{sf} \sim 2$ T for $H \parallel b$ and c and M shows a nearly H -linear increase above H_{sf} up to H_c . In a magnetic field between H_{sf} and H_c , a spin-canted magnetization process is realized and the anisotropy is expected to be small from a small magnitude of H_{sf} . Here, we should note the different relation of T_N vs H_c between two compounds. In $\text{GdRu}_2\text{Al}_{10}$, $H_c = 17$ T is roughly the same energy scale as T_N . However, in $\text{GdFe}_2\text{Al}_{10}$, $H_c = 9$ T is about half of T_N . Figure 1(f) shows the magnetic phase diagrams of $\text{GdT}_2\text{Al}_{10}$ ($T = \text{Ru}$ and Fe). The different magnitude of H_c between two compounds is clearly seen, regardless of nearly the same T_N . Thus, not only in the paramagnetic region but also in the AFM ordered phase, a largely different magnetic behavior is seen.

In $\text{LnT}_2\text{Al}_{10}$, the NN Ln ion is located on the zigzag chain along the c axis shown by solid gray lines in Fig. 2. The distance between the NN Ln ion is ~ 5.2 Å. The distance between the nearest zigzag chains is ~ 7 Å. This is rather larger than 5.2 Å. Then, it is natural to expect that the NN Gd moments on the zigzag chain orders antiferromagnetically and the two-sublattice model could be applicable. Our preliminary results of NQR (nuclear quadrupole resonance) measurements of $\text{GdRu}_2\text{Al}_{10}$ strongly suggests the commensurate magnetic order.²⁷ Then, from the experimental results shown in Fig. 1(b), m_{AFM} is expected to be along the [011] direction and two kinds

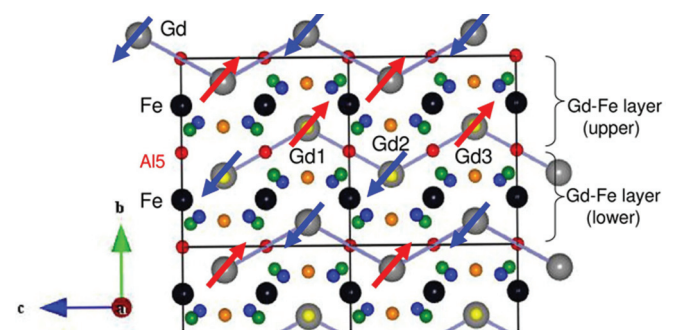


FIG. 2. (Color online) Crystal structure of $\text{LnT}_2\text{Al}_{10}$ in the bc plane. The proposed AFM structure in the ground state is shown by arrows. The two sublattices are indicated by the red and blue arrows. The solid gray lines indicate the zigzag chain along the c axis. Small circles indicate five Al sites and the Al5 site is denoted in the figure.

of domain of $m_{\text{AFM}} \parallel [011]$ and $[01\bar{1}]$ are expected. This type of AFM order is not usual. If m_{AFM} is along the b or c axis, the magnetic dipole fields on the Gd moment from two NN Gd moments are degenerate and a frustration effect is expected. When m_{AFM} is aligned in the intermediate direction in the bc plane as shown in Fig. 2, the magnetic dipole field on the Gd2 site from the Gd1 site is stronger than that from the Gd3 site. Namely, the magnetic dipole interaction between Gd1 and Gd2 is larger than that between Gd2 and Gd3. Then, there exists a tendency to form a dimerized pair on the zigzag chain in the AFM order. We estimated the magnetic dipole field on the Gd2 site from the surrounding Gd moments with $7\mu_B$ located inside the sphere with a radius of 100 Å. When the two-sublattice AFM order as shown in Fig. 2 is assumed, it is 879, 568, 310, and 458 Oe when $m_{\text{AFM}} \parallel a, b, c,$ and $[011]$, respectively. Thus, if only the magnetic dipole field is considered as the origin of the magnetic anisotropy below T_N , $m_{\text{AFM}} \parallel a$ is most favorable. This contradicts the anisotropy of χ below T_N . The magnetic dipole field for $m_{\text{AFM}} \parallel b$ is quite small. However, its component is contained in the AFM alignment. On the other hand, the order of magnitude of the observed H_{sf} is consistent with that of $\sqrt{2H_A H_{ex}}$ when the anisotropic field $H_A \sim 10^3$ Oe and the exchange field $H_{ex} \sim 10^5$ Oe. Our preliminary results of the thermal expansion of $\text{GdRu}_2\text{Al}_{10}$ indicate that the b and c axes show a shrinkage and expansion, respectively, with nearly the same magnitude, and the a axis shows a quite small shrinkage below T_N .²⁸ This means that the AFM order gets the energy gain by shrinking the b axis and the variation of the a axis is not associated with the energy gain in the AFM order. The expansion of the c axis might be a result of the shrinkage of the b axis and supports the commensurate magnetic order. Thus, the AFM order on the zigzag chain and the origin of the magnetic anisotropy are interesting problems to be clarified. The proposed AFM structure of the present compounds drawn in Fig. 2 should be examined by a microscopic experimental method in the future.

Here, we consider two kinds of AFM exchange interactions. One is the intersublattice one, J_{ex}^{AB} , and the other is the intrasublattice one, $J_{ex}^{AA}(=J_{ex}^{BB})$. The mean-field Hamiltonian is as follows. The thermal average $\langle S_x \rangle^A$, etc., were determined self-consistently.

$$\begin{aligned} \mathcal{H} &= \mathcal{H}_A + \mathcal{H}_B, \quad \mathcal{H}_A = \sum_{i \in A} h_i^A, \quad \mathcal{H}_B = \sum_{i \in B} h_i^B, \\ h_i^A &= -J_{ex}^{AB} (\langle S_x \rangle^B S_x + \langle S_y \rangle^B S_y + \langle S_z \rangle^B S_z) \\ &\quad - J_{ex}^{AA} (\langle S_x \rangle^A S_x + \langle S_y \rangle^A S_y + \langle S_z \rangle^A S_z) + H_{Zeeman}, \\ h_i^B &= -J_{ex}^{AB} (\langle S_x \rangle^A S_x + \langle S_y \rangle^A S_y + \langle S_z \rangle^A S_z) \\ &\quad - J_{ex}^{BB} (\langle S_x \rangle^B S_x + \langle S_y \rangle^B S_y + \langle S_z \rangle^B S_z) + H_{Zeeman}. \end{aligned}$$

The procedure to determine the exchange interactions is as follows. First, we determine J_{ex}^{AB} and $J_{ex}^{AA}(=J_{ex}^{BB})$ at low temperature so as to reproduce the experimental results of T_N at $H = 0$ and H_c at $T = 1.4$ K. Second, we calculate the temperature dependence of χ and χ^{-1} by using the exchange interactions obtained in the first step. Third, if they are not consistent with the experimental results, we introduce the temperature dependence of the exchange interactions. Figure 3(a) shows the calculated results of the T dependence of χ and $1/\chi$ corresponding to those of $T = \text{Ru}$ and Fe. Figures 3(b)

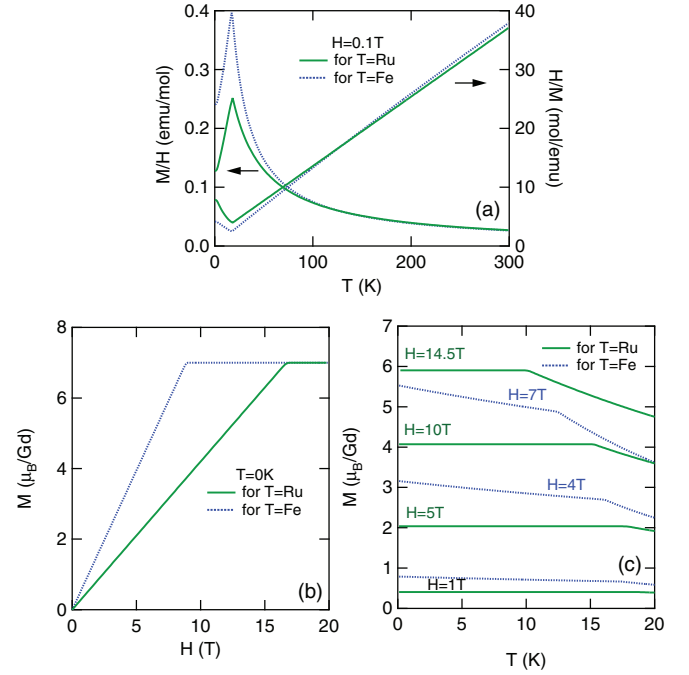


FIG. 3. (Color online) (a) Temperature dependence of χ and $1/\chi$ where H is applied along the z axis under the initial condition of $m_{\text{AFM}} \parallel [011]$ in the AFM phase, (b) magnetization curve at $T = 0$, and (c) temperature dependence of M for $T = \text{Ru}$ and Fe at low temperatures where a spin-canted state is realized below T_N calculated by a mean-field approximation.

and 3(c) show the M - H curve at $T = 0$ K and the temperature dependence of M at low temperatures, respectively.

First, we discuss the case of $\text{GdRu}_2\text{Al}_{10}$. In $\text{GdRu}_2\text{Al}_{10}$, once J_{ex}^{AB} is fixed to be -3.2 K, all the experimental results could be reproduced very well without introducing $J_{ex}^{AA}(=J_{ex}^{BB})$. Namely, $T_N = 17$ K and $H_c = 17$ T could be reproduced and the calculated χ^{-1} is very consistent with the experimental results. The calculated θ_p value of -17 K is also consistent with the experimental value of ~ -16 K. Thus, $\text{GdRu}_2\text{Al}_{10}$ could be understood as the normal AFM compound dominated only by J_{ex}^{AB} .

Next, we discuss the case of $\text{GdFe}_2\text{Al}_{10}$. In this compound, as far as only J_{ex}^{AB} is taken into account, the experimental results could not be reproduced. In order to reproduce the small magnitude of $\theta_p = 0$ K estimated below 50 K and $H_c = 9$ T, we should introduce the ferromagnetic interaction in the intrasublattice interaction $J_{ex}^{AA}(=J_{ex}^{BB})$. To reproduce the experimental results of T_N and H_c , $J_{ex}^{AB} = -1.7$ K and $J_{ex}^{AA}(=J_{ex}^{BB}) = 1.2$ K are obtained. However, the temperature dependence of χ and χ^{-1} could not be reproduced. Then, the temperature dependent exchange interactions should be taken into account to reproduce θ_p , which is varied with temperature. Thus, phenomenologically, we introduce the simple form of the temperature dependent exchange interactions as follows. $J_{ex}^{AB} = -1.7 - 2.8 \times \{1 - (300 - T)^2/300^2\}$ and $J_{ex}^{AA}(=J_{ex}^{BB}) = 1.2 \times \{(T - 300)^2/300^2\}$. Then, J_{ex}^{AB} is -4.5 K and -1.7 K at $T = 300$ and 0 K, respectively, and $J_{ex}^{AA}(=J_{ex}^{BB})$ is 0 and 1.2 K at $T = 300$ and 0 K, respectively. The experimental results of $\text{GdFe}_2\text{Al}_{10}$ also could be well reproduced by the calculation as shown in Fig. 3, apart from a discrepancy

of the temperature dependence of M at low temperatures between the experimental and calculated results shown in Fig. 3(c). This discrepancy is not serious but is expected to be reduced by a small modification of the temperature dependence of the exchange interactions at low temperatures. Thus, we conclude that two kinds of exchange interactions should be introduced and the exchange interactions should be temperature dependent in $\text{GdFe}_2\text{Al}_{10}$. *What is the origin of the temperature dependent exchange interactions in this compound?* Here, we recall the unusual magnetic properties of $\text{YFe}_2\text{Al}_{10}$, reported recently.^{23–26} Fe ion has a magnetic moment in this compound and the magnitude of Fe moment increases with decreasing temperature. $\text{YFe}_2\text{Al}_{10}$ is located in a close region of the ferromagnetic instability. On the other hand, in $\text{CeFe}_2\text{Al}_{10}$ and $\text{YbFe}_2\text{Al}_{10}$, the Fe ion does not have a moment. This is due to a large hybridization between $4f$ electrons of Ce or Yb and the $3d$ one of Fe. Thus, the Fe ion in $\text{LnT}_2\text{Al}_{10}$ is located near the boundary between localized and itinerant nature. Considering such a situation, it is natural to expect that the Fe ion in $\text{GdFe}_2\text{Al}_{10}$ has a magnetic moment as in $\text{YFe}_2\text{Al}_{10}$ and the magnitude of the Fe moment grows up with decreasing temperature. Then, it is natural to ascribe the origin of the temperature dependent exchange interaction between Gd ions to the exchange enhancement of the Fe magnetic moment which grows up with decreasing temperature. The different nature between $\text{GdRu}_2\text{Al}_{10}$ and $\text{GdFe}_2\text{Al}_{10}$ might be associated with the different magnitude of the c - f hybridization between magnetic $\text{CeRu}_2\text{Al}_{10}$ and nonmagnetic $\text{CeFe}_2\text{Al}_{10}$.

Finally, we discuss the relation between the phenomenologically introduced temperature dependent exchange interactions and the crystal structure in $\text{GdFe}_2\text{Al}_{10}$. The crystal structure of $\text{LnT}_2\text{Al}_{10}$ could be viewed as a two-dimensional structure

where a Ln-T layer in the ac plane is stacked along the b axis by way of an Al5 site.^{18,29} While the NN Gd moments on the zigzag chain are antiparallel, Gd moments in the Gd-Fe layer order ferromagnetically on the surface and they form the intrasublattice Gd moments. When the Fe moment has a tendency to order ferromagnetically as a whole, the exchange interaction between the Gd moments is affected by the Fe moment. When the Fe moment grows up with decreasing temperature, the ferromagnetic $J_{ex}^{AA}(=J_{ex}^{BB})$ is expected to increase by way of the ferromagnetic Fe moment. The same mechanism could also be applicable for the origin of the reduction of J_{ex}^{AB} with a decrease of temperature. Namely, Gd moments in the upper Gd-Fe layer are antiparallel to that in the lower Gd-Fe layer. On the other hand, Fe moment has a tendency to order ferro-magnetically in both layers. Then, the magnitude of J_{ex}^{AB} is expected to be reduced by the growing up of the ferromagnetic Fe moment. Thus, the origin of the temperature dependent exchange interactions between Gd moments are induced by the Fe moment. It is interesting to compare the properties of $\text{LnRu}_2\text{Al}_{10}$ and $\text{LnFe}_2\text{Al}_{10}$ to clarify the role of the Fe ion. The investigation of $\text{LnFe}_2\text{Al}_{10}$ is important to clarify both the nature of the Ln-Fe interaction and the origin of the different magnitude of the c - f hybridization between $\text{CeRu}_2\text{Al}_{10}$ and $\text{CeFe}_2\text{Al}_{10}$.

In summary, the magnetic properties of the AFM compound $\text{GdT}_2\text{Al}_{10}$ ($T = \text{Ru}$ and Fe) were studied. We found that the exchange interaction in $\text{GdFe}_2\text{Al}_{10}$ is varied largely with temperature, different from a simple AFM magnet, $\text{GdRu}_2\text{Al}_{10}$. We ascribed its origin to the exchange enhancement of the Fe ion with decreasing temperature as was observed in $\text{YFe}_2\text{Al}_{10}$. The magnetic anisotropy in the AFM phase could not be understood by the magnetic dipole interaction. This suggests the characteristics of the AFM order on the zigzag chain.

¹V. M. Thiede, T. Ebel, and W. Jeitsschko, *J. Mater. Chem.* **8**, 125 (1998).

²A. M. Strydom, *Physica B* **404**, 2981 (2009).

³T. Nishioka, Y. Kawamura, T. Takesaka, R. Kobayashi, H. Kato, M. Matsumura, K. Kodama, K. Matsubayashi, and Y. Uwatoko, *J. Phys. Soc. Jpn.* **78**, 123705 (2009).

⁴H. Tanida, D. Tanaka, M. Sera, C. Moriyoshi, Y. Kuroiwa, T. Takesaka, T. Nishioka, H. Kato, and M. Matsumura, *J. Phys. Soc. Jpn.* **79**, 043708 (2010).

⁵A. Kondo, J. Wang, K. Kindo, T. Takesaka, Y. Kawamura, T. Nishioka, D. Tanaka, H. Tanida, and M. Sera, *J. Phys. Soc. Jpn.* **79**, 073709 (2010).

⁶D. D. Khalyavin, A. D. Hillier, D. T. Adroja, A. M. Strydom, P. Manuel, L. C. Chapon, P. Peratheepan, K. Knight, P. Deen, C. Ritter, Y. Muro, and T. Takabatake, *Phys. Rev. B* **82**, 100405 (2010).

⁷D. T. Adroja, A. D. Hillier, P. P. Deen, A. M. Strydom, Y. Muro, J. Kajino, W. A. Kockelmann, T. Takabatake, V. K. Anand, J. R. Stewart, and J. Taylor, *Phys. Rev. B* **82**, 104405 (2010).

⁸J. Robert, J.-M. Mignot, G. Andre, T. Nishioka, R. Kobayashi, M. Matsumura, H. Tanida, D. Tanaka, and M. Sera, *Phys. Rev. B* **82**, 100404 (2010).

⁹J. Robert, J.-M. Mignot, S. Petit, P. Steffens, T. Nishioka, R. Kobayashi, M. Matsumura, H. Tanida, D. Tanaka, and M. Sera, *Phys. Rev. Lett.* **109**, 267208 (2012).

¹⁰S. I. Kimura, T. Iizuka, H. Miyazaki, A. Irizawa, Y. Muro, and T. Takabatake, *Phys. Rev. Lett.* **106**, 056404 (2011).

¹¹H. Tanida, D. Tanaka, M. Sera, S. Tanimoto, T. Nishioka, M. Matsumura, M. Ogawa, C. Moriyoshi, Y. Kuroiwa, J. E. Kim, N. Tsuji, and M. Takata, *Phys. Rev.* **84**, 115128 (2011).

¹²K. Kunimori, M. Nakamura, H. Nohara, H. Tanida, M. Sera, T. Nishioka, and M. Matsumura, *Phys. Rev. B* **86**, 245106 (2012).

¹³H. Tanida, D. Tanaka, Y. Nonaka, M. Sera, M. Matsumura, and T. Nishioka, *Phys. Rev. B* **84**, 233202 (2011).

¹⁴H. Tanida, D. Tanaka, Y. Nonaka, S. Kobayashi, M. Sera, T. Nishioka, and M. Matsumura, *Phys. Rev. B* **88**, 045135 (2013).

¹⁵A. Kondo, J. Wang, K. Kindo, Y. Ogane, Y. Kawamura, S. Tanimoto, T. Nishioka, D. Tanaka, H. Tanida, and M. Sera, *Phys. Rev. B* **83**, 180415 (2011).

¹⁶A. Kondo, K. Kindo, K. Kunimori, H. Nohara, H. Tanida, M. Sera, R. Kobayashi, T. Nishioka, and M. Matsumura, *J. Phys. Soc. Jpn.* **82**, 054709 (2013).

¹⁷Y. Muro, K. Motoya, Y. Saiga, and T. Takabatake, *J. Phys. Soc. Jpn.* **78**, 083707 (2009).

- ¹⁸M. Sera, D. Tanaka, H. Tanida, C. Moriyoshi, M. Ogawa, Y. Kuroiwa, T. Nishioka, M. Matsumura, J. Kim, N. Tsuji, and M. Takata, *J. Phys. Soc. Jpn.* **82**, 024603 (2013).
- ¹⁹I. Ishii, Y. Suetomi, H. Muneshige, S. Kamikawa, T. Fujita, S. Tanimoto, T. Nishioka, and T. Suzuki, *J. Phys. Soc. Jpn.* **81**, 064602 (2012).
- ²⁰G. Morrison, N. Haldoarachchinge, D. P. Young, and J. Y. Chan, *J. Phys.: Condens. Matter* **24**, 356002 (2012).
- ²¹Y. Muro, J. Kajino, T. Onimaru, and T. Takabatake, *J. Phys. Soc. Jpn.* **80**, SA021 (2011).
- ²²M. Reehuis, M. W. Wolff, A. Krimmel, E-W. Scheidt, N. Stusser, A. Loidl, and W. Jeitschko, *J. Phys.: Condens. Matter* **15**, 1773 (2003).
- ²³A. M. Strydom and P. Peratheepan, *Phys. Status Solidi* **4**, 356 (2010).
- ²⁴K. Park, L. S. Wu, Y. Janssen, M. S. Kim, C. Marques, and M. C. Aronson, *Phys. Rev. B* **84**, 094425 (2011).
- ²⁵A. M. Strydom, P. Peratheepan, R. Sarkar, M. Baenita, and F. Steglich, *J. Phys. Soc. Jpn.* **80**, SA043 (2011).
- ²⁶P. Khuntia, A. M. Strydom, L. S. Wu, M. C. Aronson, F. Steglich, and M. Baenitz, *Phys. Rev. B* **86**, 220401 (2012).
- ²⁷M. Matsumura (unpublished).
- ²⁸M. Sera (unpublished).
- ²⁹H. Tanida, D. Tanaka, M. Sera, C. Moriyoshi, Y. Kuroiwa, T. Takesaka, T. Nishioka, H. Kato, and M. Matsumura, *J. Phys. Soc. Jpn.* **79**, 063709 (2010).